PIV Measurements and Computational Study of Aeroacoustics of a Drone Propeller

Jianwei Sun[1], Ryo Aoki[1], Koichi Yonezawa[2, 3], and Hao Liu[1, 3(*)]

1 Graduate School of Engineering, Chiba University, Japan
2 Central Research Institute of Electrical Power Industry, Japan
3 Center for Aerial Intelligent Vehicles, Chiba University, Japan

Outline

- Background and Motivation
- Objective and Methodology
- Comparison
  - Flow field
  - Acoustic performance
  - Aerodynamic performance
- Conclusion

Background and Motivation

- Drone propellers rely on aerodynamic and aeroacoustic performance for optimal flight.
- Predicting these performance characteristics accurately is a significant challenge.
- Improving our ability to predict their performance will allow us to design more efficient and effective drone propellers.

Background and Motivation

Experiment	CFD simulation
Quantitative description of flow phenomena using measurement	Quantitative prediction of flow phenomena using CFD software
For a quantity at a time	For all desired quantities
High frequency resolution	High time resolution
For a limited range of problems and operating conditions	Virtual problems
uncertainty	Not 100 % reliable
Expensive and slow	Cheap(er) and fast(er)

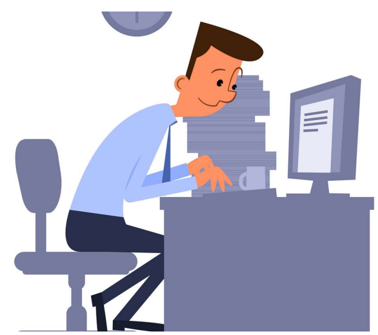

Objective and Methodology

Free-run and phase-locked PIV:

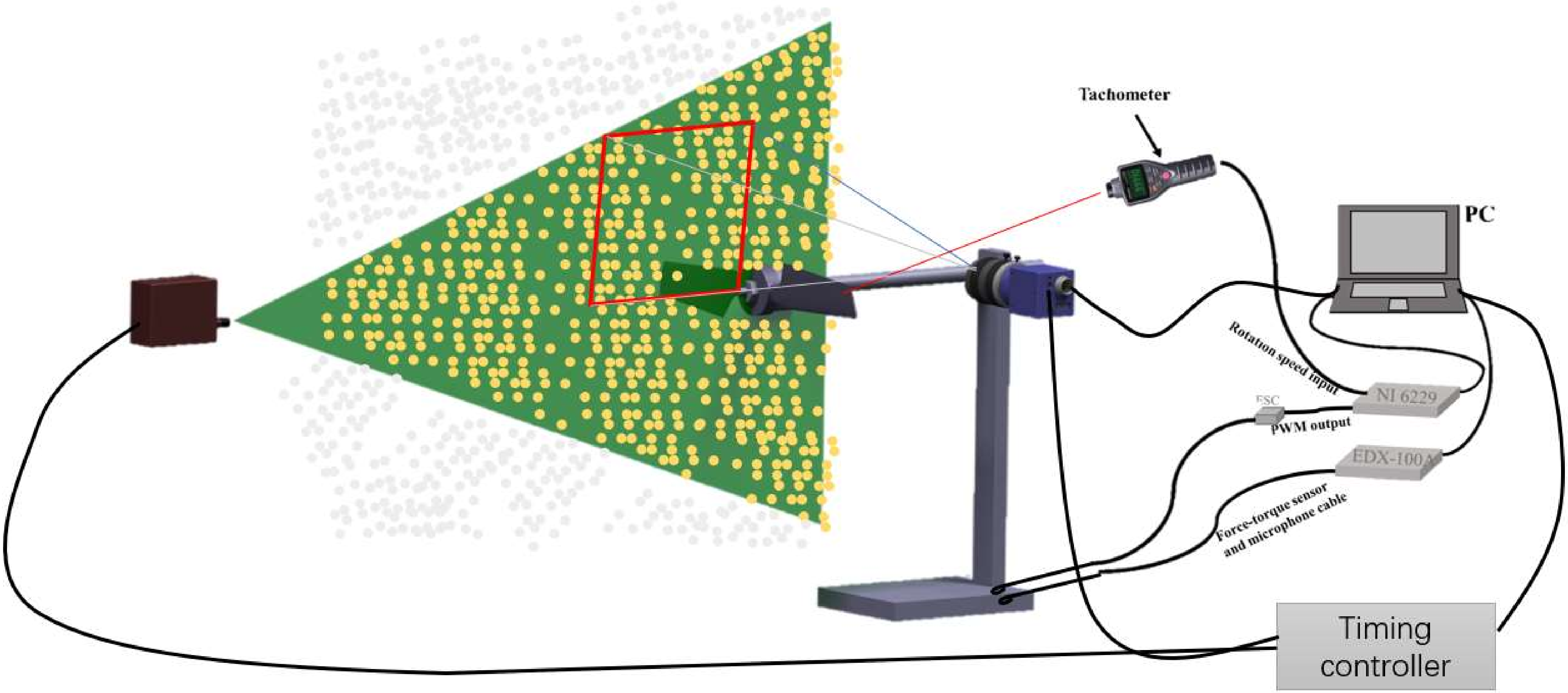

Objective and Methodology

Free-run and phase-locked PIV:

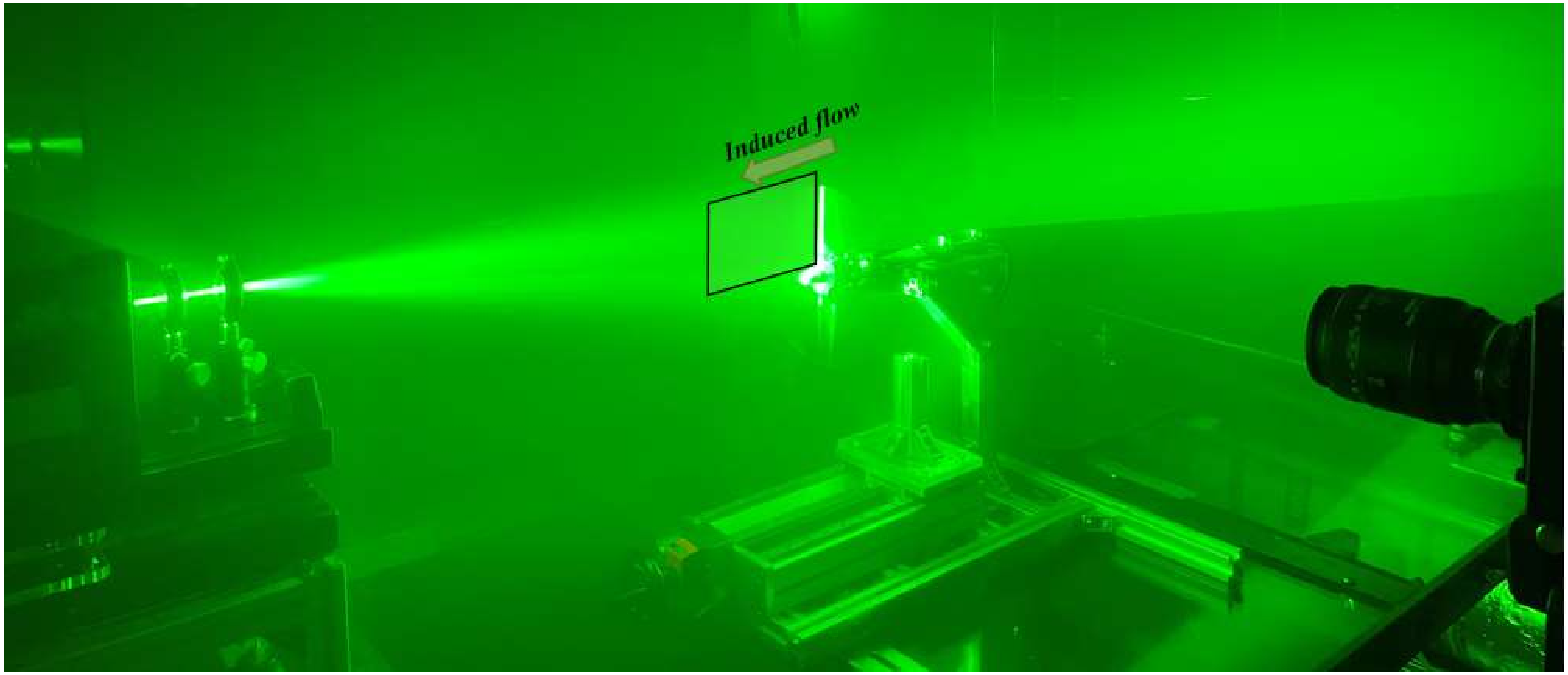

Particles on Smoke → Illuminate of laser → High-speed camera photography → Images processing

Objective and Methodology

Free-run and phase-locked PIV:

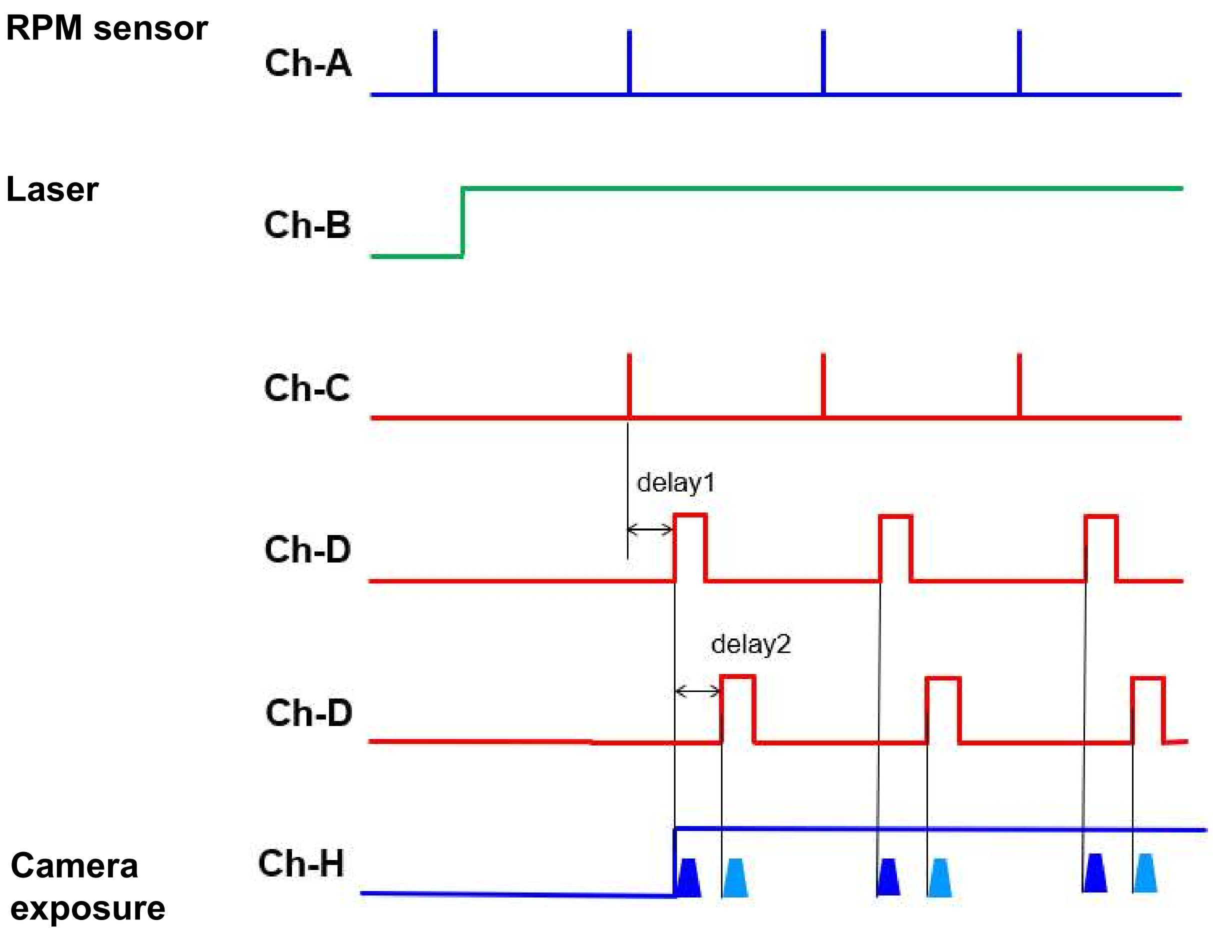

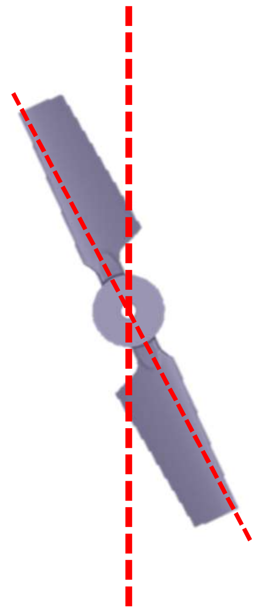

Objective and Methodology

Free-run and phase-locked PIV :

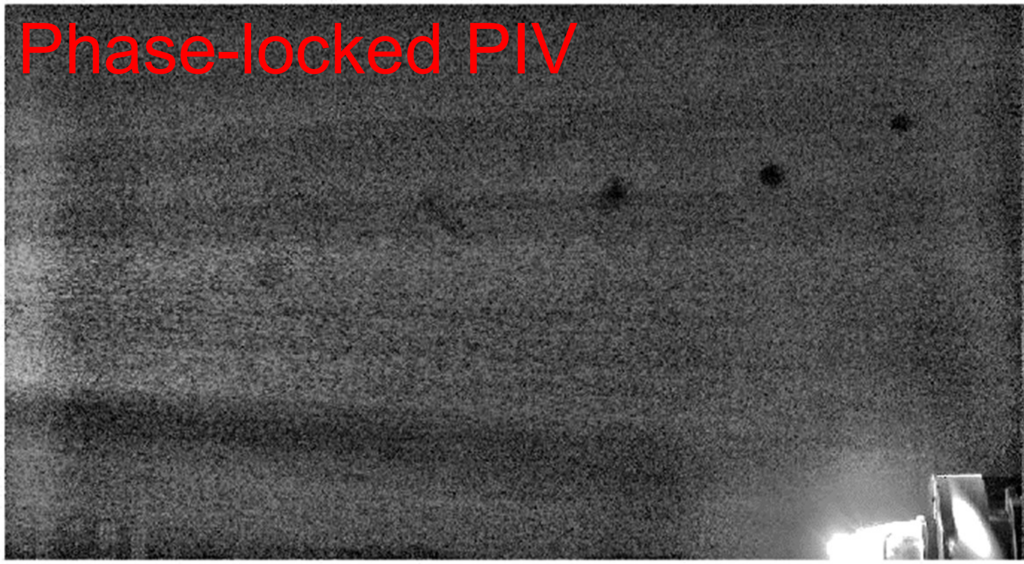

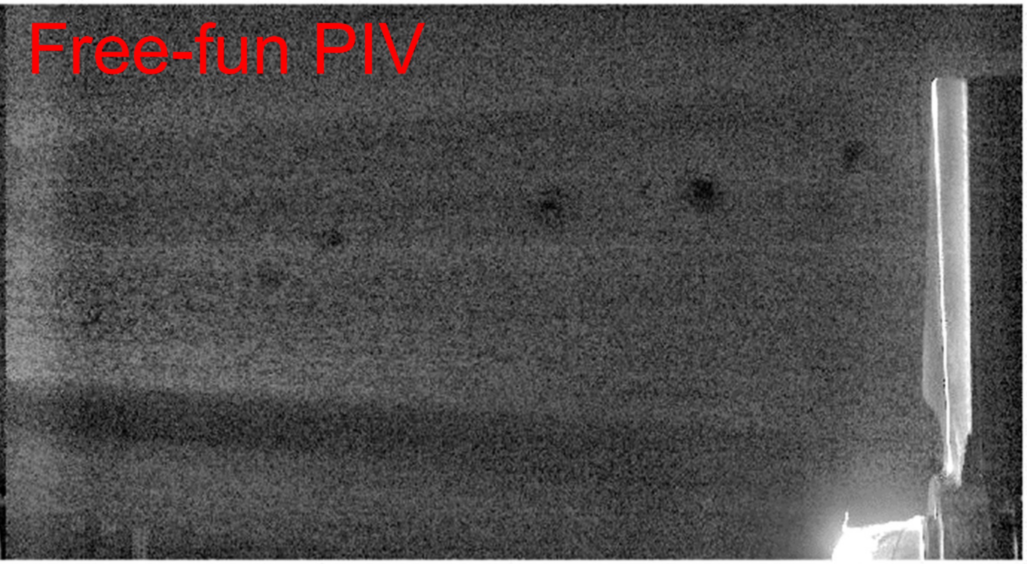

Phase-averaged

$$\bar{v} = \frac{1}{N}\sum_{i=1}^{N} v(t_0 + i\,T)$$

Time-averaged

$$\hat{v} = \frac{1}{N}\sum_{i=1}^{N} v(t_0 + i\,\Delta t)$$

- Phase-averaged algorithm: Enhances the periodic component of the signal with a known period in RPS, and filters out the random component.
- Time-averaged algorithm: Filters both the periodic and random components of the signal, but retains the trend component.

Objective and Methodology

Hover-stand experiment in anechoic chamber:

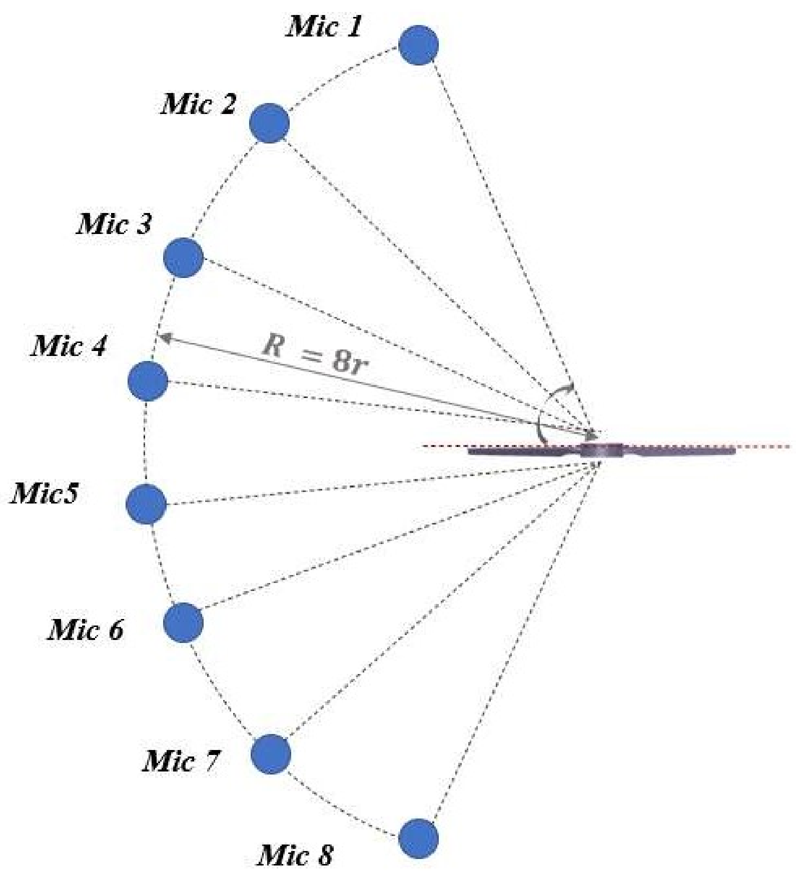

Key parameters:

Rotational speed	5400rpm
Diameter	200mm
Pitch angel	14deg
Fs(Hz) Sampling rate	50,000Hz/20,000Hz
Distance	800mm
Polar angle	75deg (mic1) & 50deg (mic2) & 25deg(mic3) & 5deg (mic4) & -5deg (mic5) & -25deg (mic 6) & -50deg (mic7) & -75deg (mic8)

Objective and Methodology

rFlow3D & rNoise:

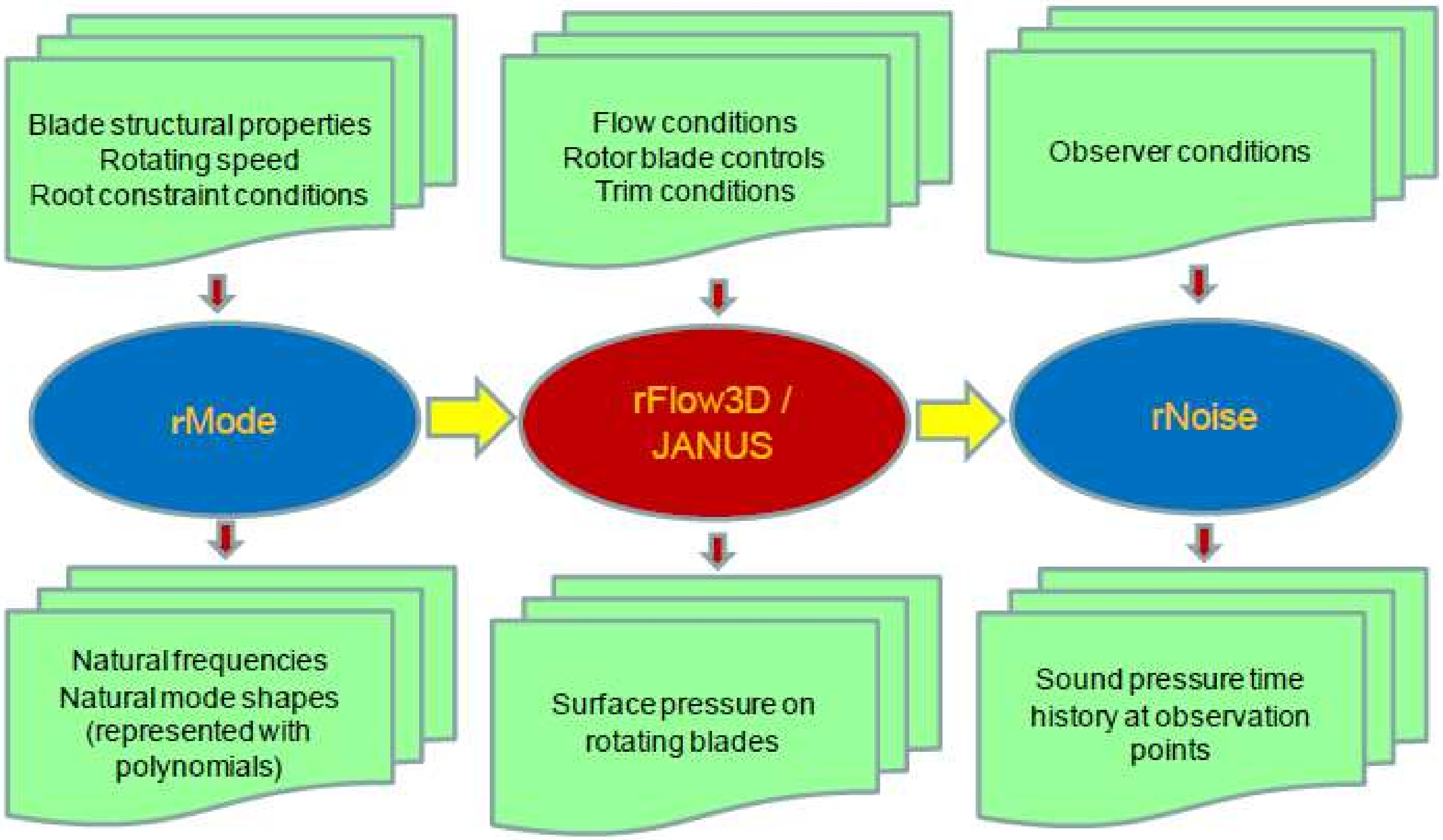

Tanabe, et. al.(2012)

Objective and Methodology

rFlow3D & rNoise:

$$\boxed{\begin{aligned} &4\pi p'(\boldsymbol{x},t) = 4\pi(p'_T(\boldsymbol{x},t) + p'_L(\boldsymbol{x},t)) = \\ &\quad \frac{\partial}{\partial t}\int_{f=0}\left[\frac{\rho_0 v_n}{r(1-M_r)} + \frac{p\cos\theta}{c\,r(1-M_r)}\right]_{ret} dS + \int_{f=0}\left[\frac{p\cos\theta}{r^2(1-M_r)}\right]_{ret} dS \end{aligned}}$$

$$4\pi p_{\mathrm{TF}}(\boldsymbol{r}_{\mathrm{ob}},t) = \frac{\partial}{\partial t}\int_{f=0}\left[\frac{\rho_0 \boldsymbol{v}_n}{r(1-M_r)}\right]_{\tau} \mathrm{d}S(\boldsymbol{r}_{\mathrm{b}})$$

Thickness noise

$$4\pi p_{\mathrm{LF}}(\boldsymbol{r}_{\mathrm{ob}},t) = \frac{1}{c_s}\frac{\partial}{\partial t}\int_{f=0}\left[\frac{p_{\mathrm{b}}\cos\theta}{r(1-M_r)}\right]_{\tau} \mathrm{d}S(\boldsymbol{r}_{\mathrm{b}})$$

Far field loading noise

$$4\pi p_{\mathrm{LN}}(\boldsymbol{r}_{\mathrm{ob}},t) = \int_{f=0}\left[\frac{p_{\mathrm{b}}\cos\theta}{r^2(1-M_r)}\right]_{\tau} \mathrm{d}S(\boldsymbol{r}_{\mathrm{b}})$$

Near field loading noise

Farassat, et. al.(2007)

Objective and Methodology

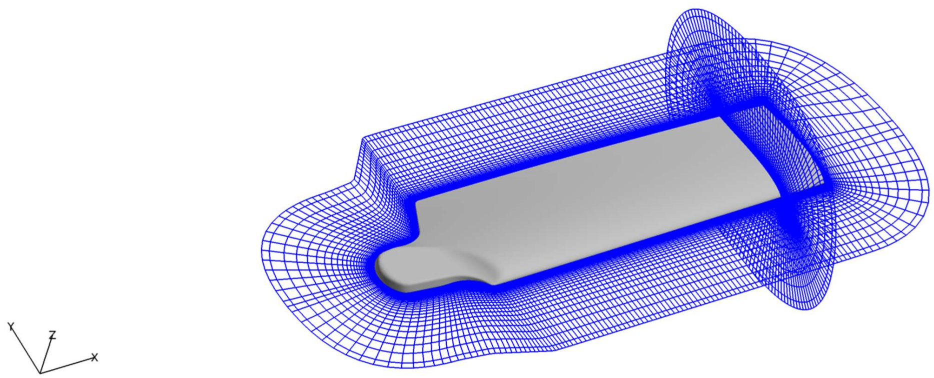

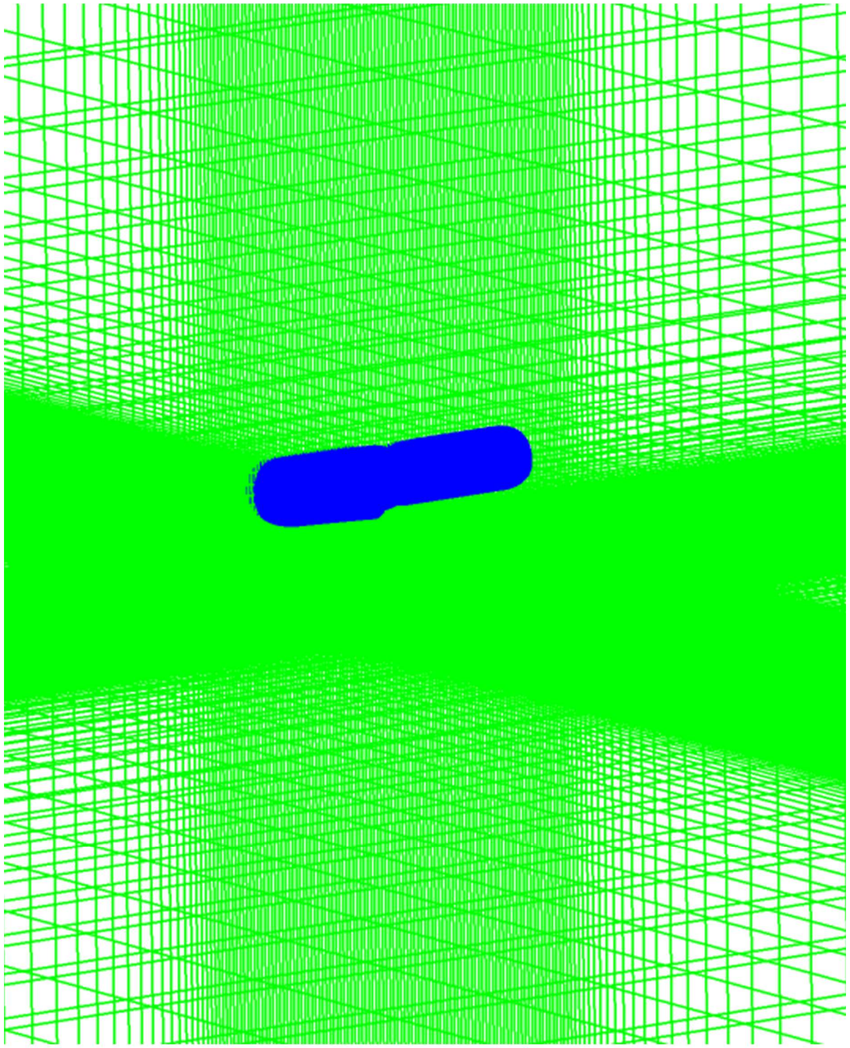

Rotational speed	5400rpm
Diameter	200mm
Pitch angel	14deg
background	**195*195*147(X*Y*Z)**
Blade grid(each)	**121*143*61**
M_TURB_IG	**0**
Output number(Msd)	1024
Fs(Hz)	92,160

Comparison – FLOW field (phase-average)

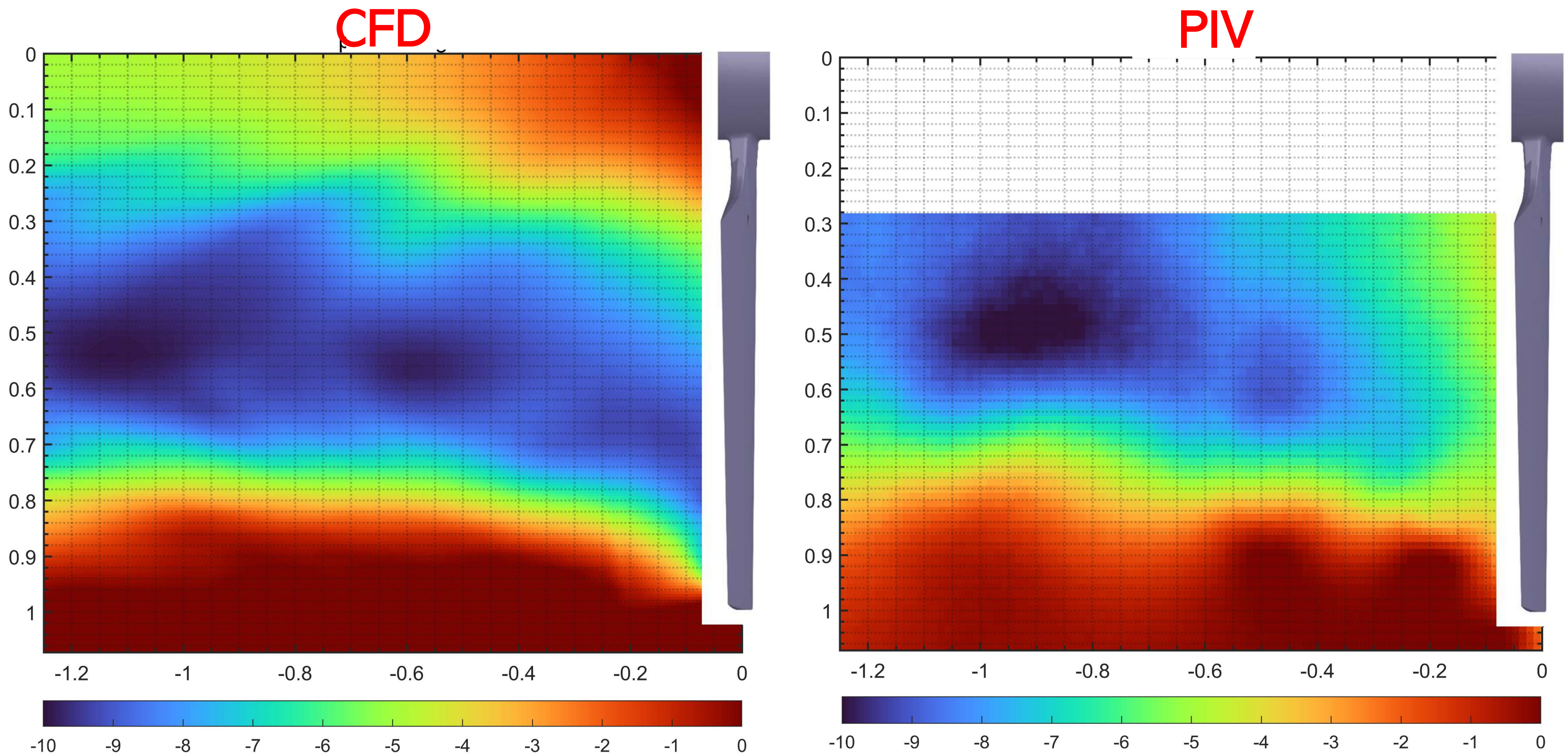

- Our phase-averaged results present the velocity fluctuation in the slipstream of the drone propeller, which can inform future design improvements.

Comparison – FLOW field (time-average)

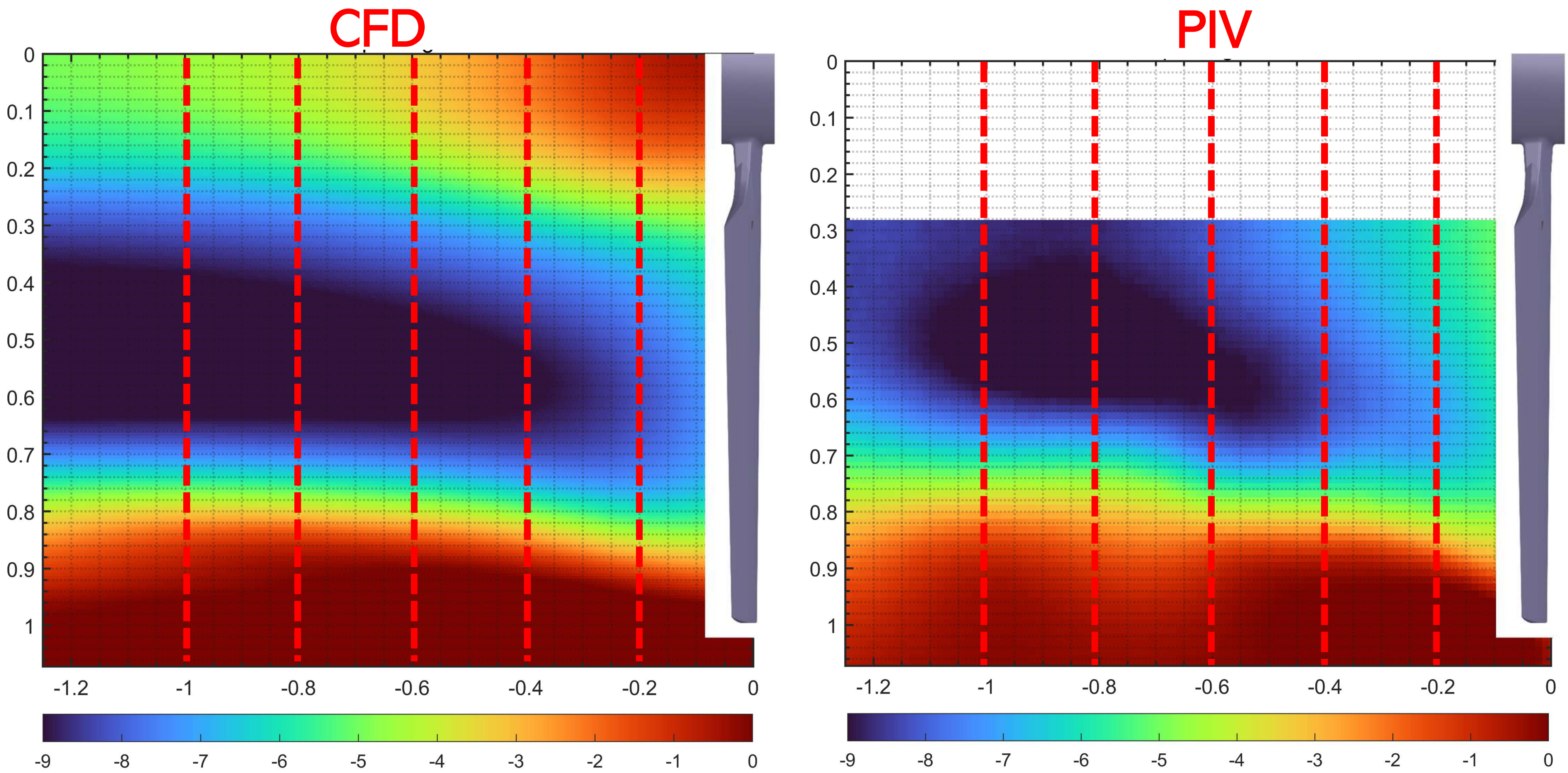

- Time-averaged result shows reasonable agreement in the slipstream between PIV and CFD methods, providing confidence in the accuracy of our methods and results.

Comparison – FLOW field (time-average)

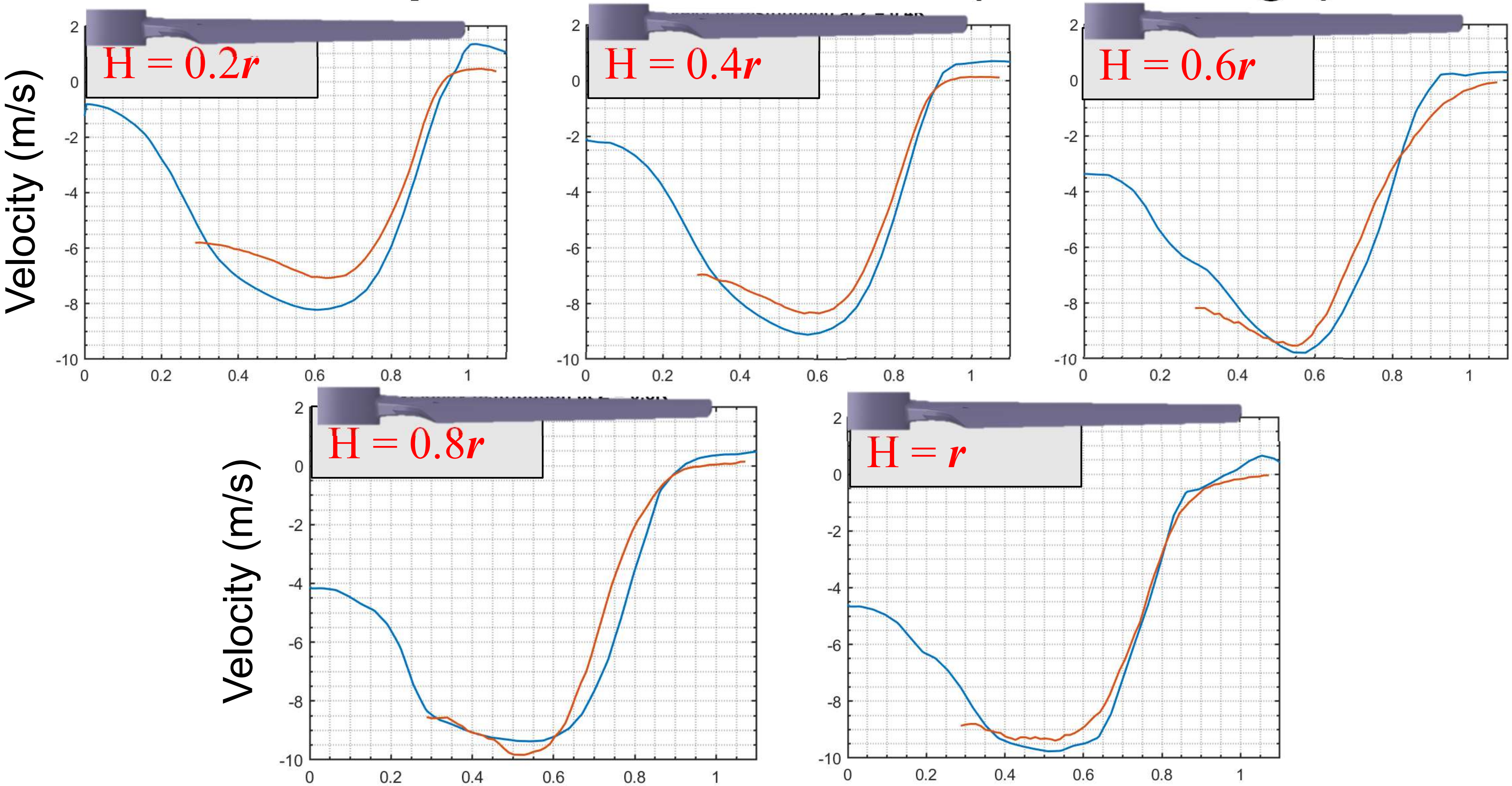

- Comparison of velocity distribution at different planes parallel to the rotational plane between CFD and PIV shows good agreement, with slight discrepancies at H = 0.2r and 0.4r.

Comparison – FLOW field (time-average)

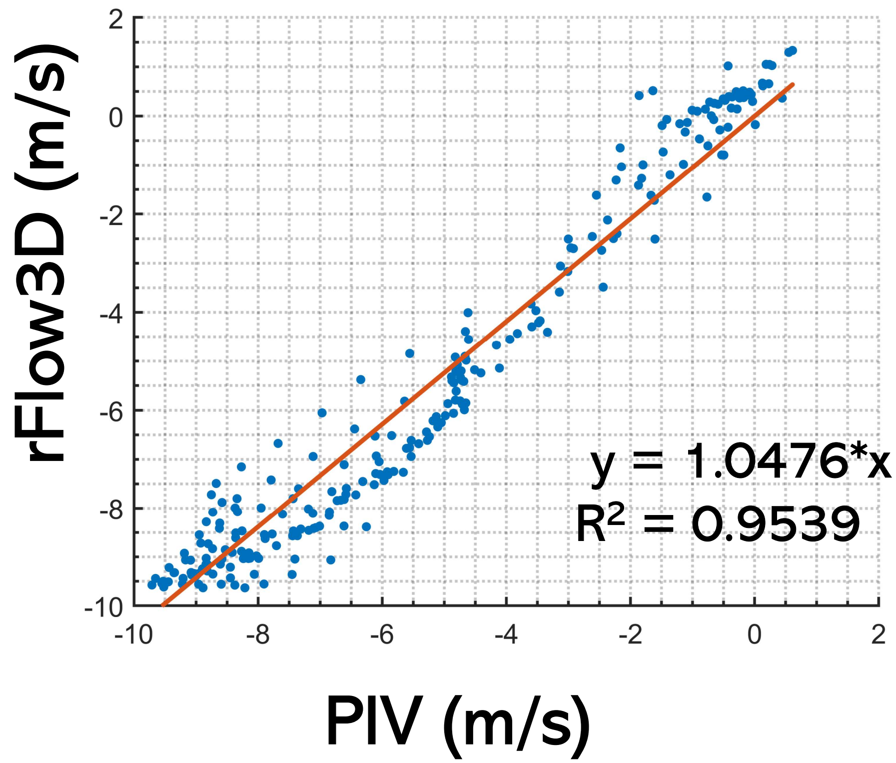

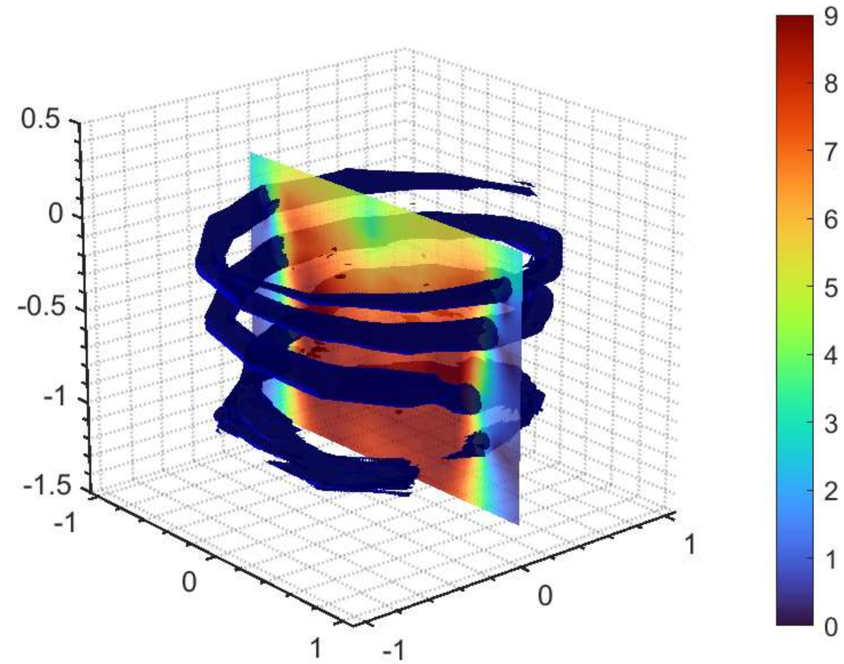

PIV measurement

- The high R-squared value obtained between the time-averaged results of PIV and CFD methods indicates a good agreement between the two methods in terms of the velocity values.

Comparison – acoustic

Overall SPL SIM. vs. EXP.

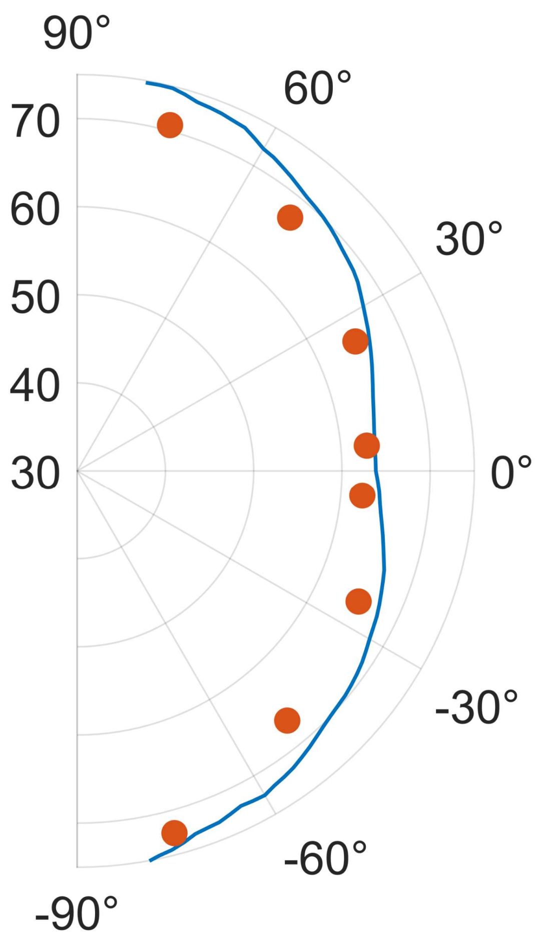

simulation

experiment

< 3.2dB

- Our comparison of predicted and experimental OASPL results shows good agreement, with a difference of less than 3.2 dB

Comparison – acoustic

Overall SPL SIM. vs. EXP.

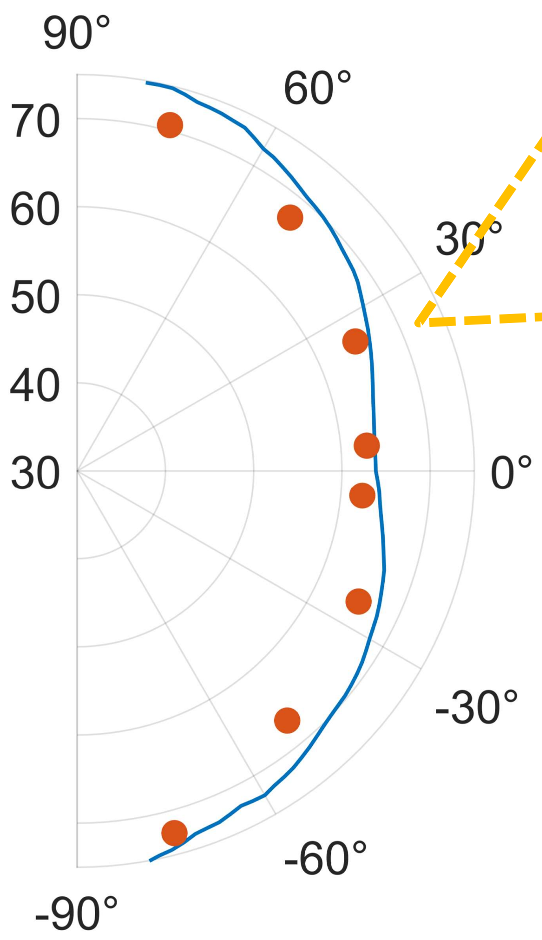

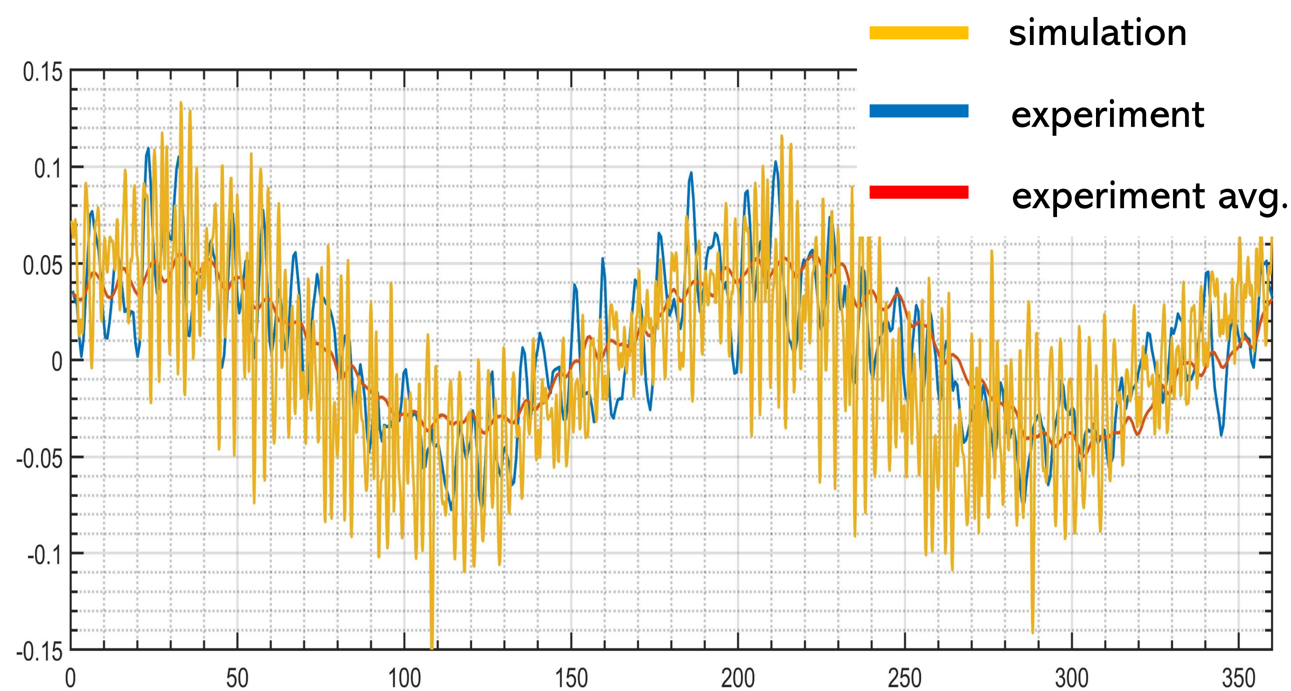

64.8dB (exp.) vs 66.2 dB (sim.)

- A similar trend between the predicted and experimental results in the time domain, especially at blade passing frequency (BPF), although the simulation result has more high-frequency noise.

Comparison – acoustic

Overall SPL SIM. vs. EXP.

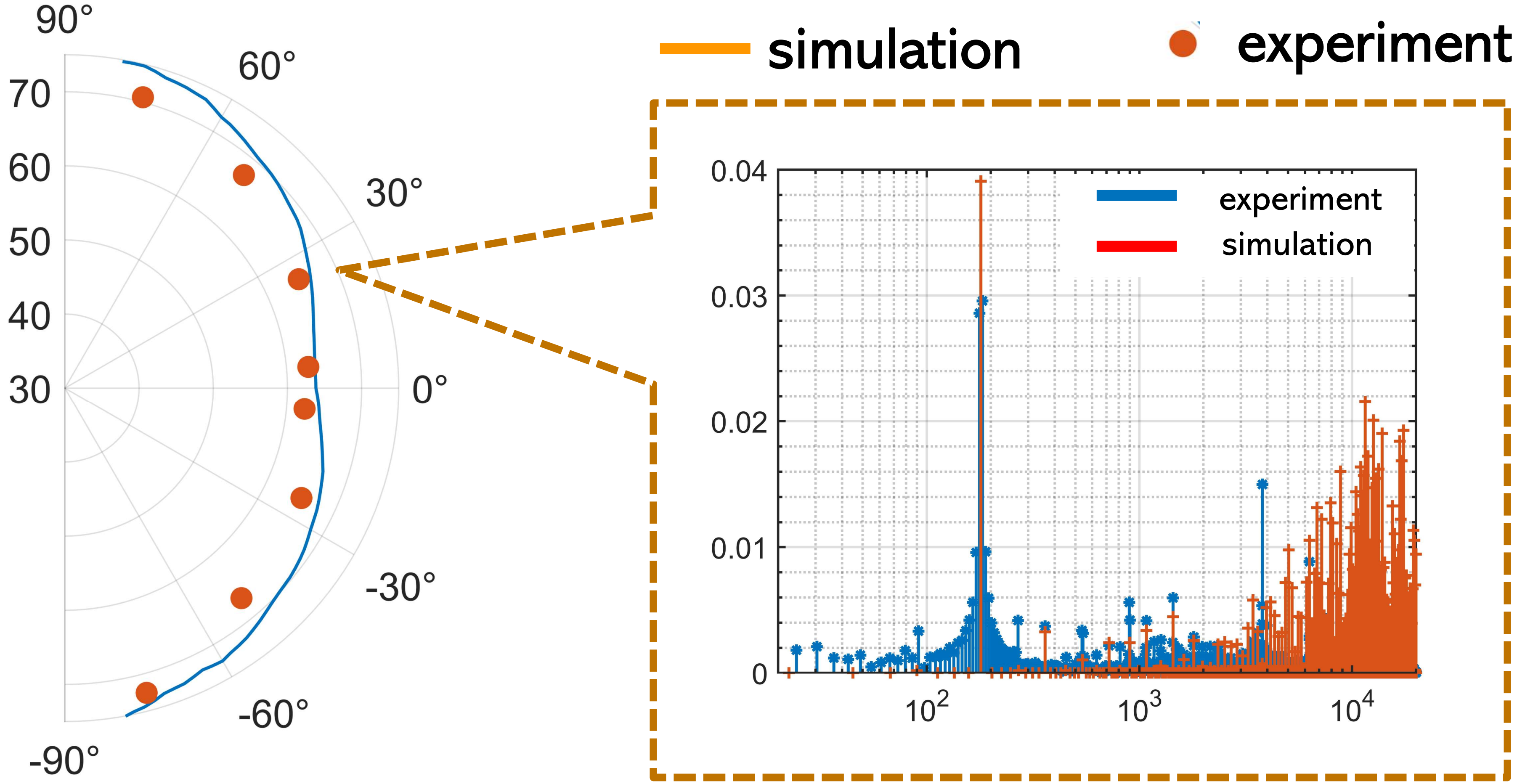

- Our frequency analysis confirms that the CFD model predicts more high-frequency noise than the experimental result.

Comparison – acoustic

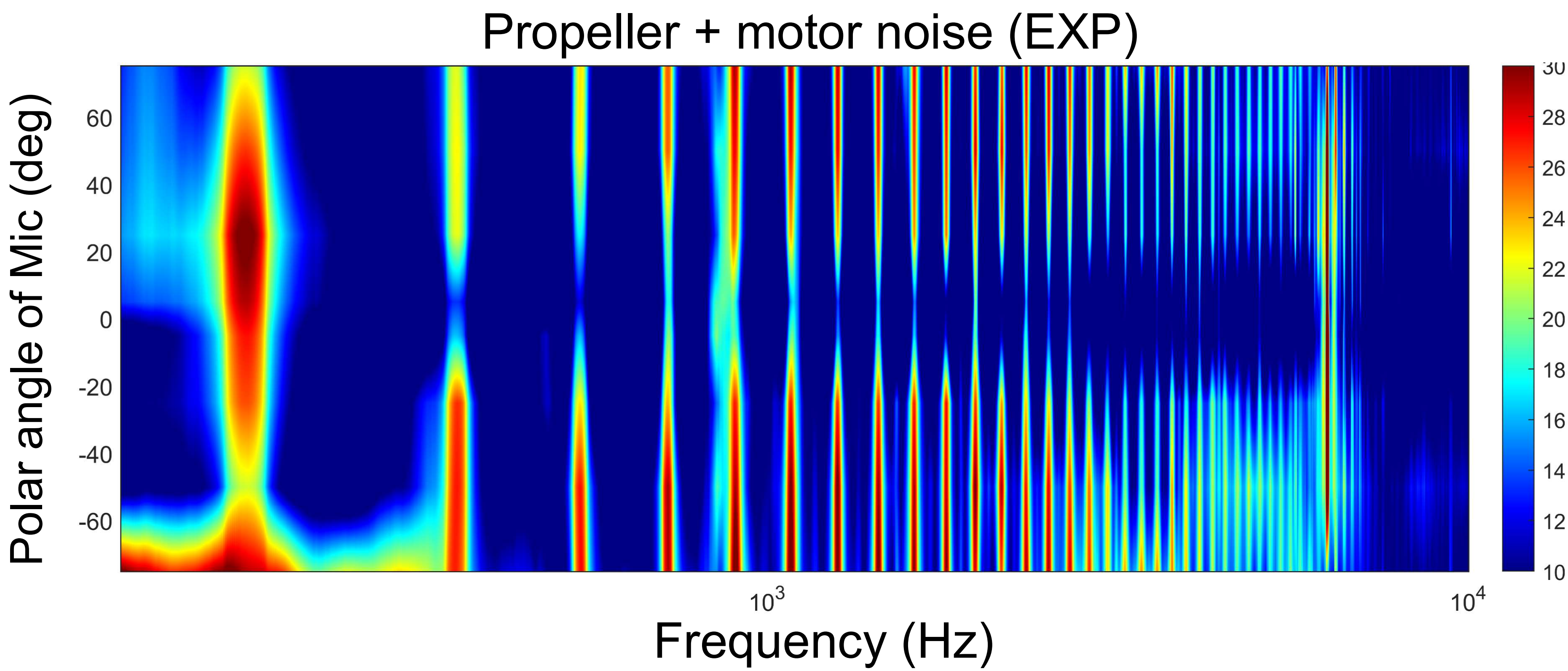

- The noise SPL at the BPF of the propeller reveals that the noise level is higher at lower polar angles, while the high-frequency noise is higher at higher polar angles.

Comparison – acoustic

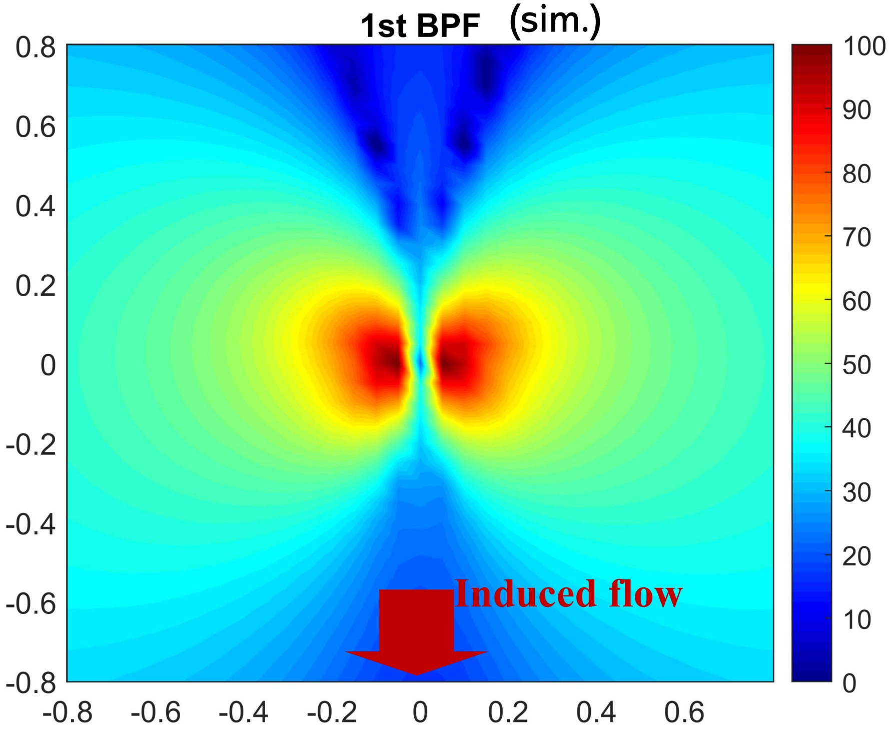

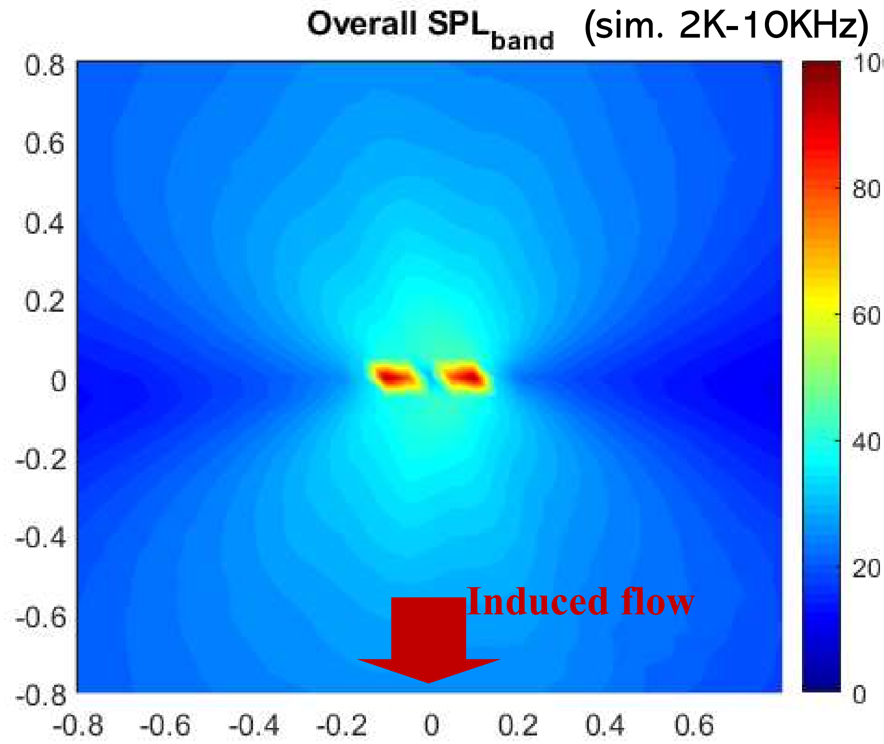

- The CFD simulations predict the similar noise emission pattern with the experimental result.

Comparison – acoustic

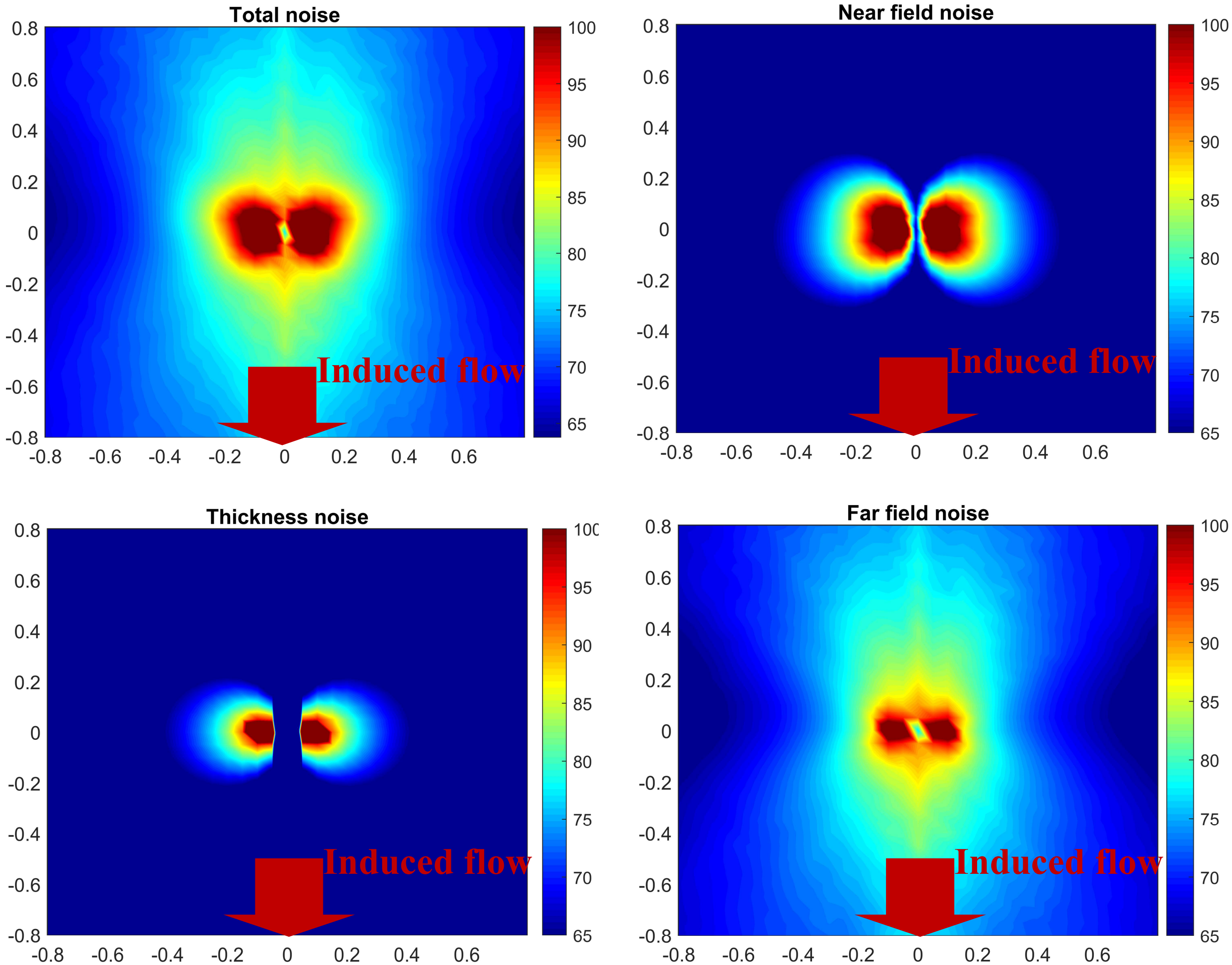

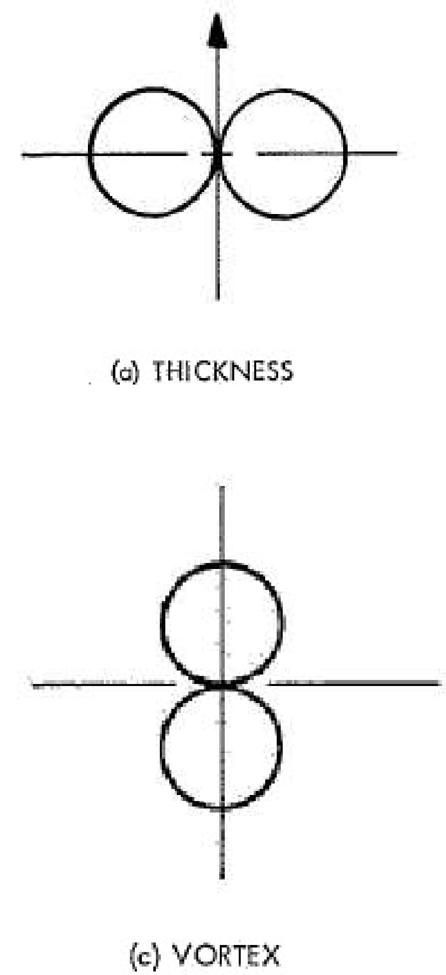

- The rFlow3D/rNoise simulations predict the similar noise emission pattern with the theoretical result.

Made, et. al.(1970)

Comparison – acoustic

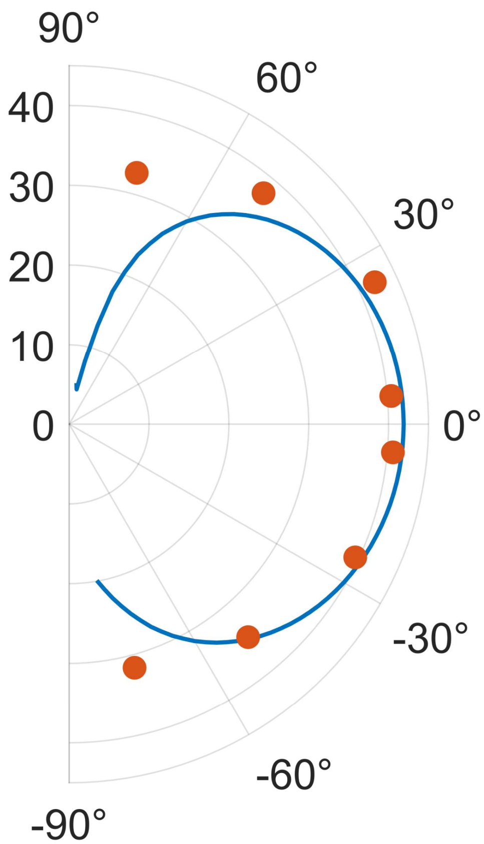

1st BPF SPL

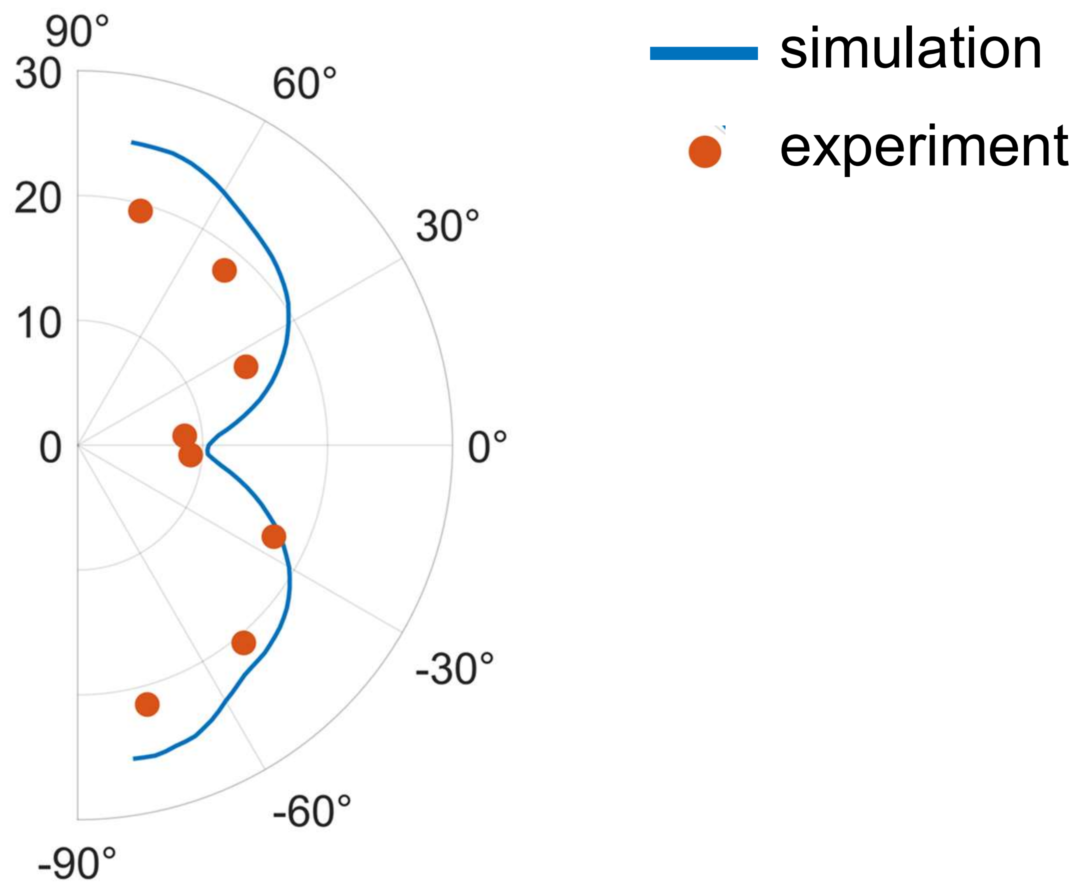

$OASPL_{band}$ (2K-10K)

Comparison – acoustic

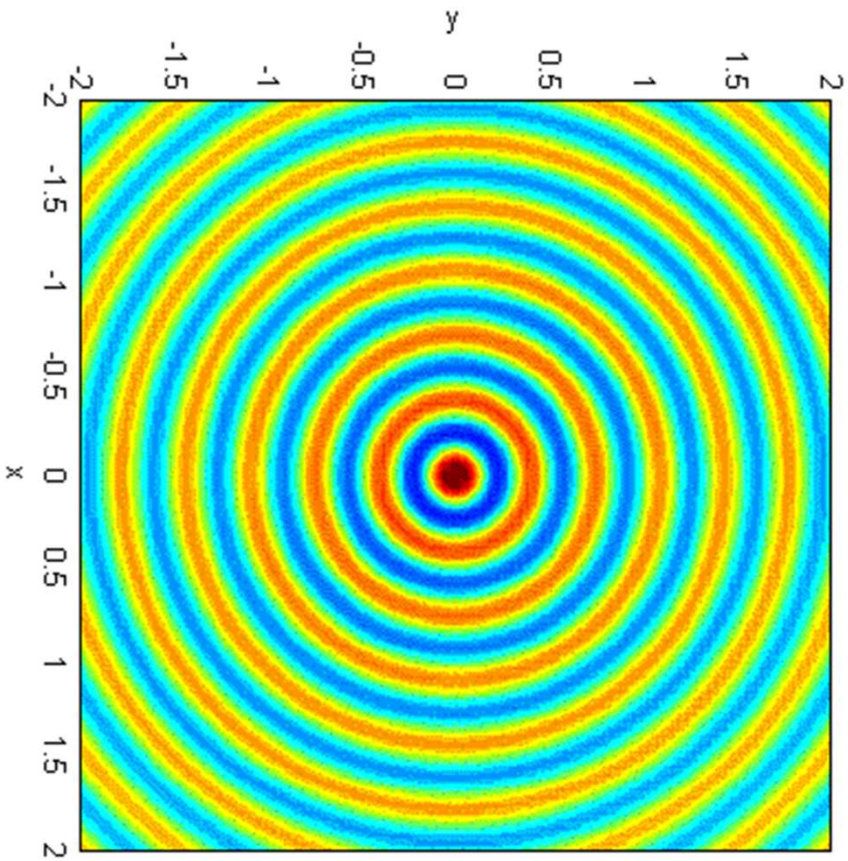

Monopole

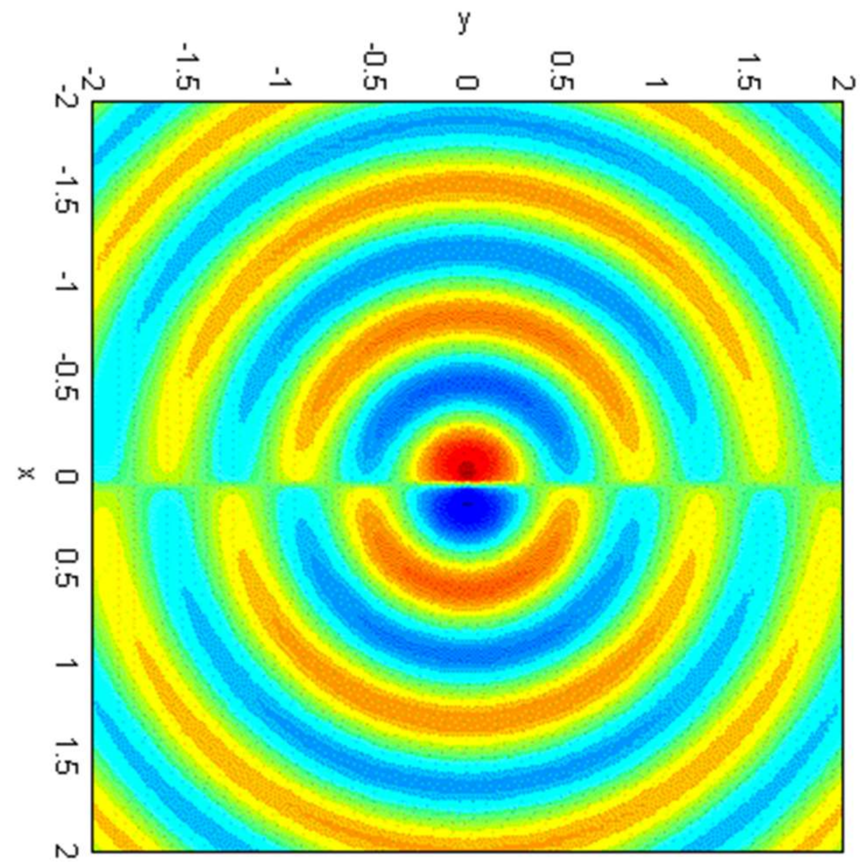

Dipole

- Acoustic Radiator Models: Monopole model and Dipole model.

https://en.wikibooks.org/wiki/Aeroacoustics/Acoustic_Sources

Comparison – acoustic

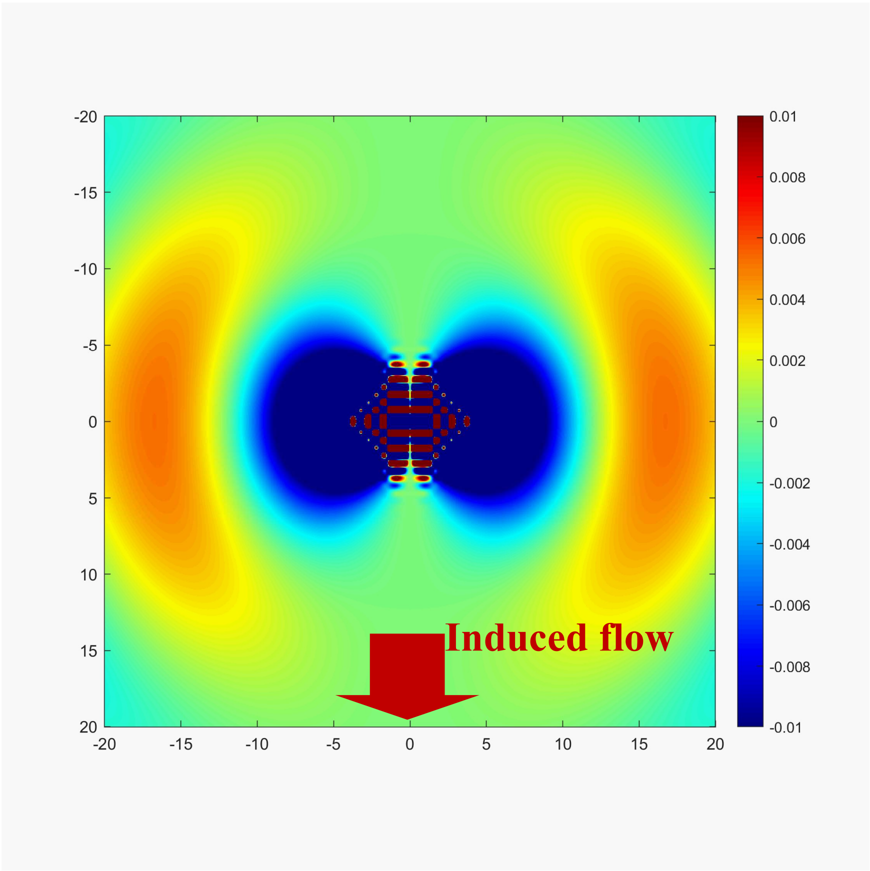

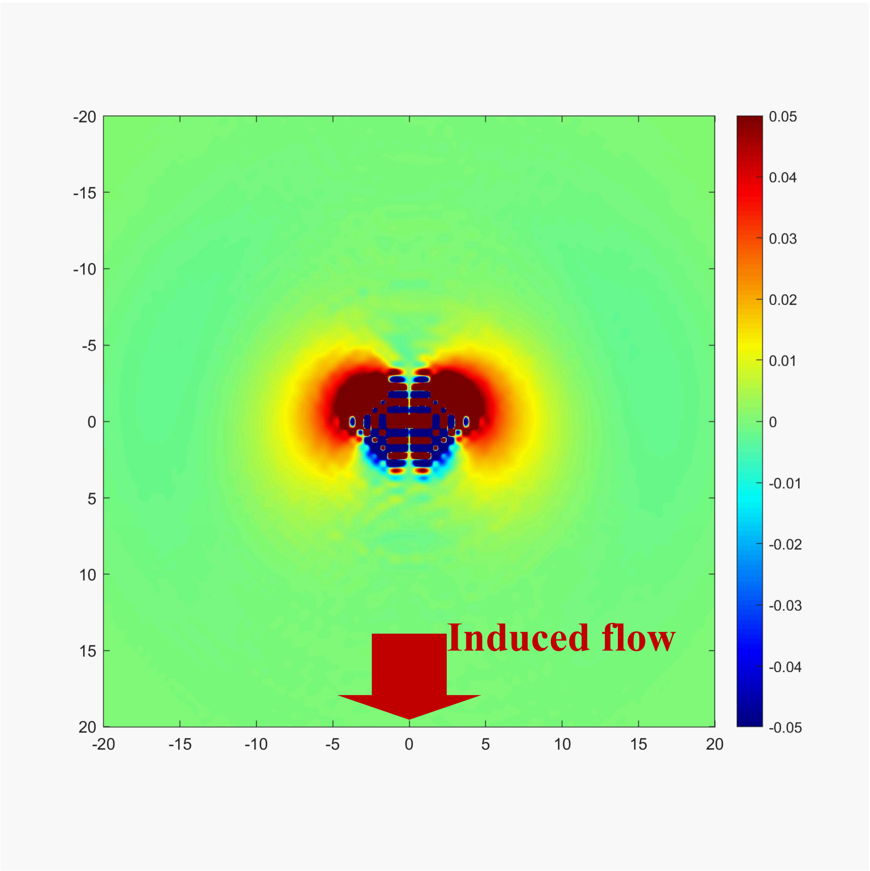

Thickness noise-Monopole

Loading noise (near)-Dipole

- The rFlow3D/rNoise simulations predict the sound source emission pattern in time scale.

Comparison – acoustic

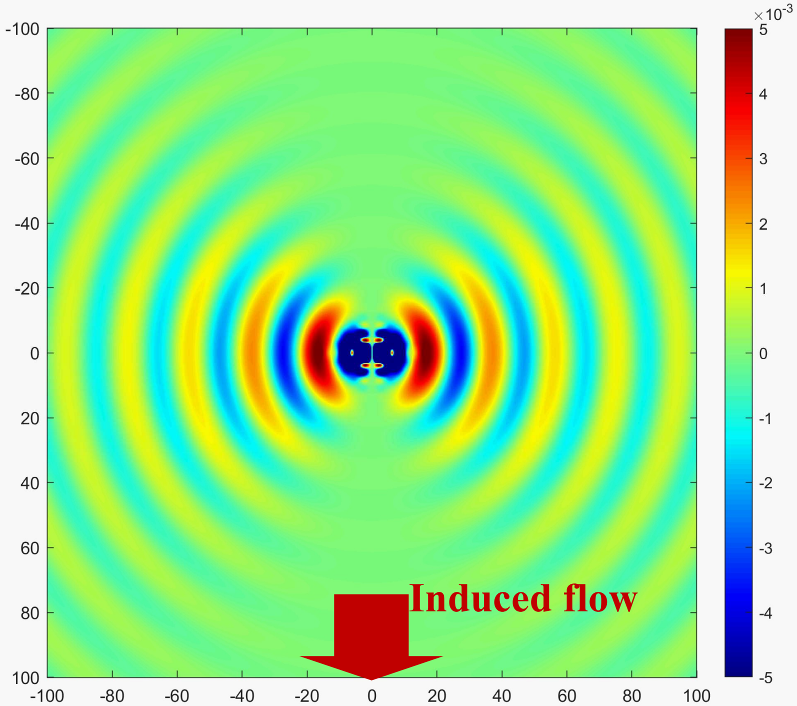

Thickness noise-Monopole

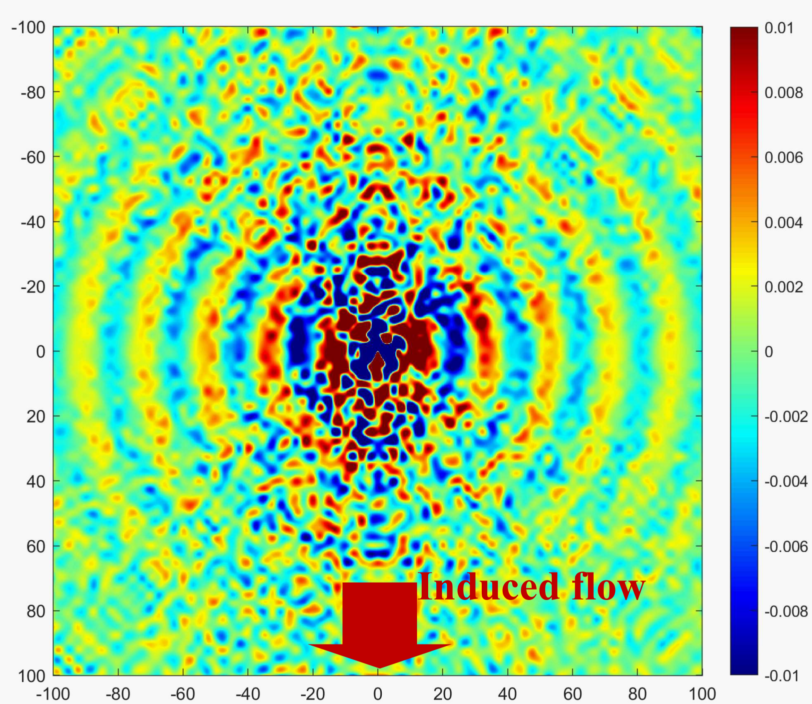

Total noise (PTF + PNL+PFL)

- The rFlow3D/rNoise simulations result explain that the tonal noise is enhanced at lower polar angle, broadband noise is enhanced at higher polar angle.

Comparison – Aerodynamic performance

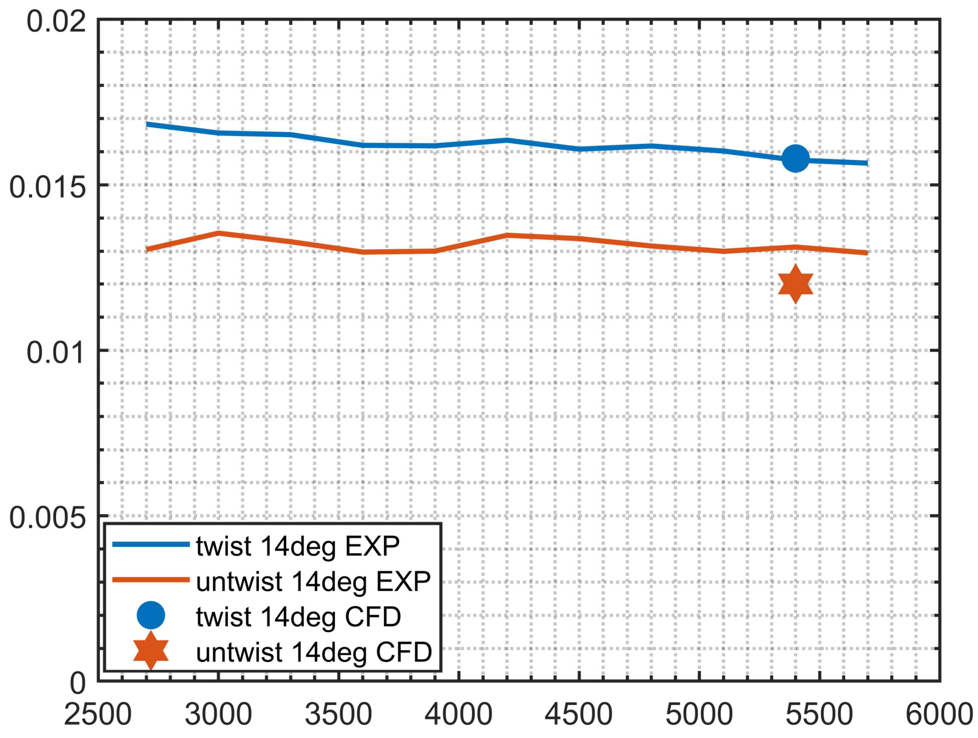

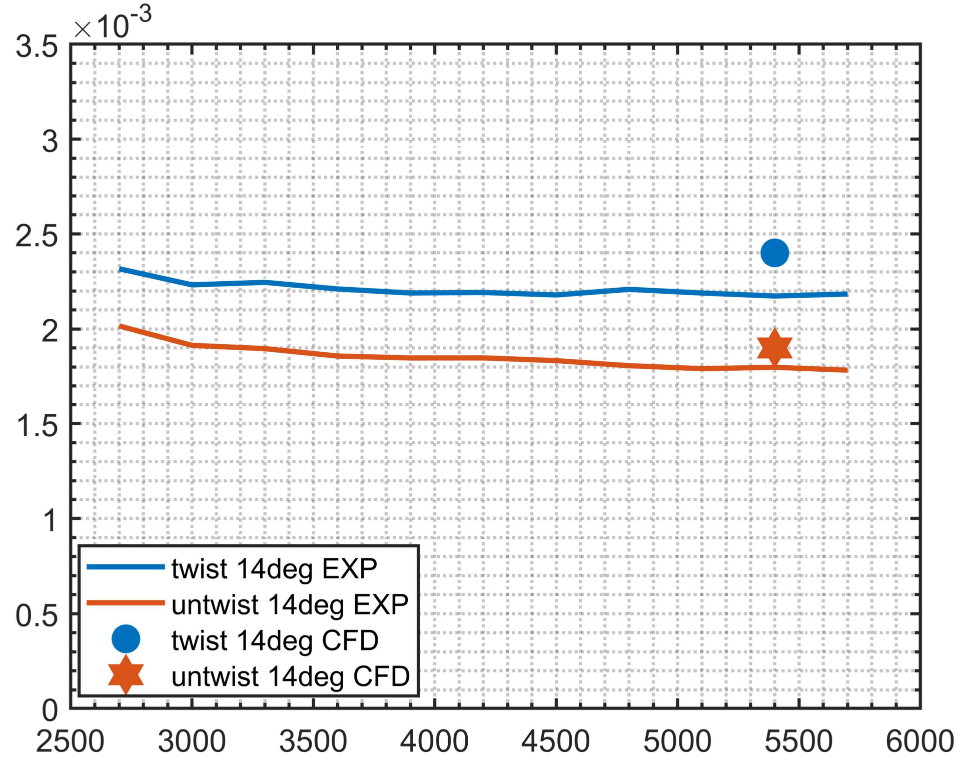

< 6.5%

< 8.0%

- The evaluation of aerodynamic forces using rFlow3D shows an error rate of less than 8%

Conclusion

- The results indicate that rFlow3D produces flow field velocity data that is consistent with PIV measurement, as verified by goodness-of-fit analysis.
- However, it should be noted that *rFlow3D/rNoise* may introduce an overestimation of noise levels in positions where the polar angle is greater than 60 degrees due to the influence of higher frequency components. Nonetheless, the patterns of noise emission observed align with theoretical predictions and experimental evidence.
- Furthermore, the evaluation of aerodynamic forces using rFlow3D shows an error rate of less than 8%, which is acceptable. These findings suggest that rFlow3D is a reliable tool for analyzing aerodynamic performance.